Laboratory Intercomparison of the Ozone Absorption Coefficients in the Mid-infrared (10 μm) and Ultraviolet (300−350 nm) Spectral Regions

B. Picquet-Varrault,*,† J. Orphal,‡ J.-F. Doussin,† P. Carlier,† and J.-M. Flaud‡

Laboratoire Interuniversitaire des Systèmes Atmosphériques, UMR-CNRS 7583, University of Paris 7 and Paris 12, 94010 Créteil cedex, France, and Laboratoire de Photophysique Moléculaire, UPR-CNRS 3361, 91405 Orsay cedex, France

Received: August 11, 2004

For the measurement of atmospheric ozone concentrations, the mid-infrared and ultraviolet regions are both used by ground-, air-, or satellite-borne instruments. In this study we report the first laboratory intercomparison of the ozone absorption coefficients using simultaneous measurements in these spectral regions. The intercomparison shows good agreement (around 98.5%) between the HITRAN 2000 recommendation for the mid-infrared and the most reference measurements in the ultraviolet regions, whereas systematic differences of about 5.5% are observed when using the recommendation of HITRAN2003 for the mid-infrared. Possible reasons for this discrepancy are discussed. Future measurements are clearly needed to resolve this issue.

1. Introduction

The determination of accurate molecular transition moments is a challenging task. While for energy levels, relative experimental uncertainties of less than 10^{-9} are achieved without great difficulty, the measurement of line intensities or absorption cross-sections is still limited to relative uncertainties of several 10^{-2}. Furthermore, accurate transition moments are not only of importance for molecular physics, for example to understand intramolecular dynamics, but in particular for atmospheric chemistry and remote sensing, where relatively small variations of atmospheric trace gas concentrations need to be monitored. In many cases, the accuracy of available laboratory measurements is the main contribution to the overall error budget of atmospheric remote-sensing experiments.

Ozone is one of the most important molecules in the terrestrial atmosphere since it filters the solar ultraviolet (UV) radiation and plays a key role in the atmospheric photochemistry. To have a good understanding of the physical and chemical processes in which it is involved, very accurate atmospheric concentration profiles are required.

For this reason, many ground-based, air-borne, balloon-borne, or satellite measurements of ozone are performed routinely using spectrometers working in the UV−visible, infrared, and microwave spectral ranges. In particular recently the European satellite ENVISAT has been launched with two spectrometers on board, SCIAMACHY ("Scanning Imaging Absorption Spectrometer for Atmospheric Chartography") for measurements in the UV−visible spectral region and MIPAS ("Michelson Interferometer for Passive Atmospheric Sounding") for measurements in the thermal infrared.

In the mid-infrared range, the 10-μm band of ozone is very strong and is the most widely used to derive atmospheric concentration profiles. In the UV region, the Huggins bands are currently used for spectroscopic remote sensing of ozone by many experimental techniques (Dobson and Brewer spectrometers, differential optical absorption spectroscopy using zenith-sky observations, etc). In both cases in order to obtain accurate ozone concentration profiles, knowledge of the absorption cross-sections is of the utmost importance. Hence, a large number of experimental determinations of the ozone absorption cross-sections have been performed using various techniques (see ref 1 and references therein).

Concerning the infrared region, the 10-μm ozone bands have been subject to numerous spectroscopic studies.[2−7] A recent review[8] of the four most recent data sets has shown that three of the experimental sets[4,6,7] agree to better than 2%, whereas the last one[5] is consistently 4.4% higher. Consequently, this review suggested using the line intensities derived from these three new data to perform atmospheric ozone retrievals. Concerning the Huggins region, many cross-section data have been published in the literature,[9−15] but significant differences due to differences in spectral resolutions and wavelength shifts were observed (about 10%).[16] However, the agreement between selected experimental studies[9,11−13] is very good (about 1−2%).[1,16]

Prior to the present study, there have been several intercomparisons of ozone absorption cross-sections in the UV and mid-infrared regions, showing an agreement better than 5%, but these studies have always been performed using the absorption of ozone at the single wavelength of 254 nm in the peak of the Hartley band.[2,4,5] On the other hand, no experimental study has ever verified the consistency between the cross-sections in the Huggins region (300−350 nm) and in the mid-infrared around 10 μm, preventing meaningful comparisons of ozone concentration profiles obtained by spectrometric measurements in the Huggins and 10-μm spectral regions.

Therefore, the aim of this study is to intercompare, for the first time, the ozone absorption coefficients in the 10-μm and the 300−350-nm regions in order to validate their consistency and check whether the published spectroscopic data in the two spectral regions are in agreement. Such a comparison has been performed by acquiring simultaneously UV and infrared spectra at room temperature and atmospheric pressure using a common optical cell.

* Corresponding author. Telephone: 33 (1) 45 17 15 90. Fax: 33 (1) 45 17 15 64. E-mail: picquet@lisa.univ-paris12.fr.
† Laboratoire Interuniversitaire des Systèmes Atmosphériques.
‡ Laboratoire de Photophysique Moléculaire.

10.1021/jp0405411 CCC: $30.25
Published on Web 01/25/2005

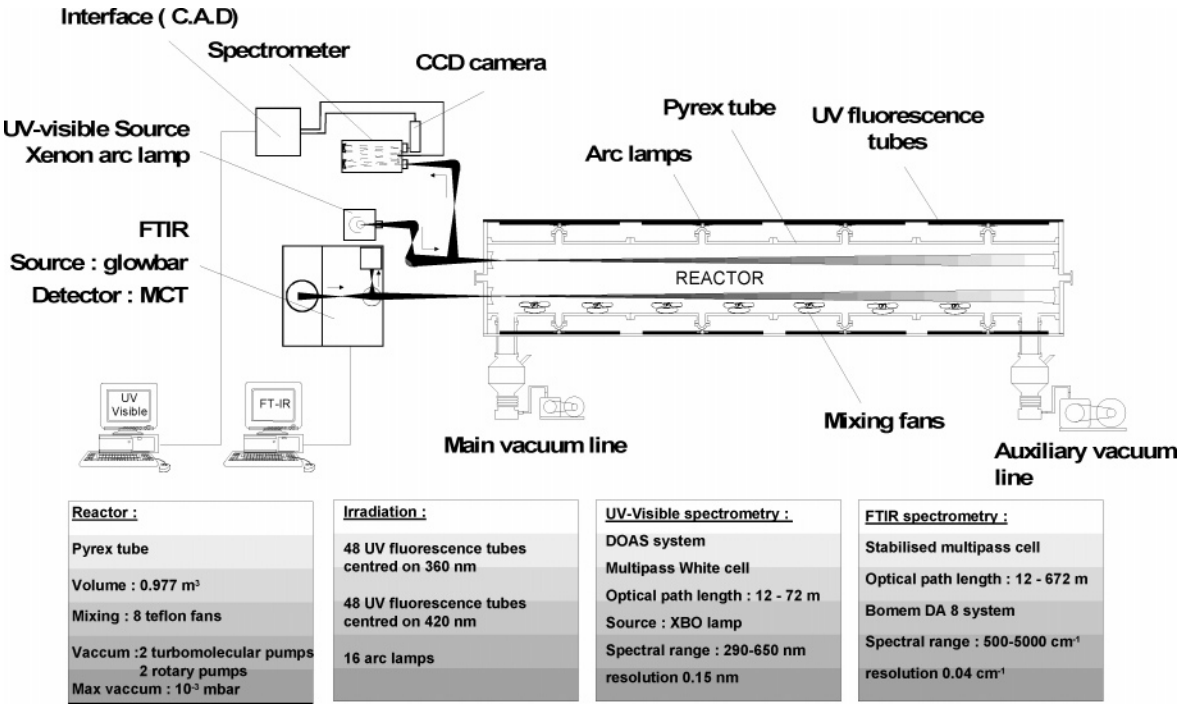

Figure 1. General setup of the reactor and spectrometers.

2. Experimental Section

2.1. Experimental Setup. The experiments were performed using an evacuable Pyrex photoreactor (6 m long; volume, 977 L) at room temperature and atmospheric pressure. This reactor contains two multiple reflection optical systems interfaced to a Fourier transform infrared (FTIR) spectrometer and to an UV−visible absorption spectrometer (see Figure 1).

UV−Visible Channel. The UV−visible channel consists of a source, a "divided-beam" optical device, a multipass cell, a monochromator, and a CCD camera as detector. The source, the optical parts, and the detector are set up on an optical table fixed on the framework and stabilized with rubber shock absorbers.

The source is a xenon high-pressure arc lamp. It is a 450-W ozone-free XBO lamp (Osram), which provides an intense ultraviolet and visible spectrum. The spectrometer is made of a Czerny−Turner monochromator (HR 320, Jobin-Yvon) and a CCD camera (CCD 3000, Jobin-Yvon). The focal length of the monochromator is 0.32 m and is equipped with a 1200 g·mm^{-1} grating. The CCD camera is made of 1024 × 58 silicon pixels, enabling the simultaneous detection of 1024 spectral elements (corresponding to a spectral range of 60 nm). It is cooled with liquid nitrogen to 243 K. The complete configuration allows us to acquire spectra from 290 to 650 nm with a maximum resolution of 0.15 nm. The apparatus function is a Gaussian function of 0.16 nm full width at half-maximum (fwhm), as validated by measurements of atomic emission lines in the relevant spectral range.

The "divided-beam" system has been developed to correct the intensity variations of the XBO lamp during the experiments, i.e., between the time when the reference spectrum I_0 is acquired (before introduction of ozone into the reactor) and the time when spectrum I is acquired (after introduction of ozone into the reactor). This optical system is shown in Figure 2. It is made of mirrors and beam splitters, which allow splitting the beam in two parts: one part enters the optical cell for the measurement and the other one stays outside to follow the XBO intensity variations. Finally, the two beams are simultaneously detected on the CCD (one above the other; see Figure 3). The correction procedure is presented in section 2.2.

The multireflection cell allows the light to make many traversals of the reactor by successive reflections on three mirrors. This cell has already been described by Doussin et al.[17] and is only briefly presented here. The mirrors of the White cell are made of aluminum and have been coated with $AlMgF_2$. The average reflectivity of this coating is 83% in the UV region, enabling an optimal maximum optical path length of 72 m (base length, 600 ± 1.0 cm). For this study, the optical path lengths used were set to 24, 48, and 72 m, depending on the experiment and the spectral region studied.

IR Channel. The infrared spectra were recorded with a Fourier transform spectrometer (BOMEM DA8-ME). The experimental setup uses a glowbar as a source, a KBr beam splitter, and an HgCdTe detector. This spectrometer allows one to perform measurements between 600 and 4000 cm^{-1} with a resolution varying from 64 to 0.013 cm^{-1} (unapodized). The spectrometer is coupled to the multireflection White-cell reactor. The cell windows are 5 mm thick, wedged by 0.6° and made of KBr. The mirrors of the cell are "hard" gold-coated and have an average reflectivity of 97%. This allows one a significantly larger number of reflections than for the UV device. For the experiments performed in this study, the spectra were recorded with a resolution of 0.08 cm^{-1}, corresponding to a maximum optical path difference of 12.6 cm and using a "Hamming" function for apodization. As for the UV channel, several optical paths were used for this study in order to measure significant and UV-compatible absorbances. The optical path lengths used in the infrared were 12, 36, 60, and 156 m (base length, 599.7 ± 1.0 cm).

2.2. Experimental Procedure. Before each series of experiments, a strict procedure for cleaning the Pyrex reactor was carried out: the reactor was filled with about 50 mbar of an O_3/O_2 mixture, and the mixture was irradiated using mercury UV photolysis lamps (located inside the reactor) during 2 days. After that, the reactor was pumped during 1 day using

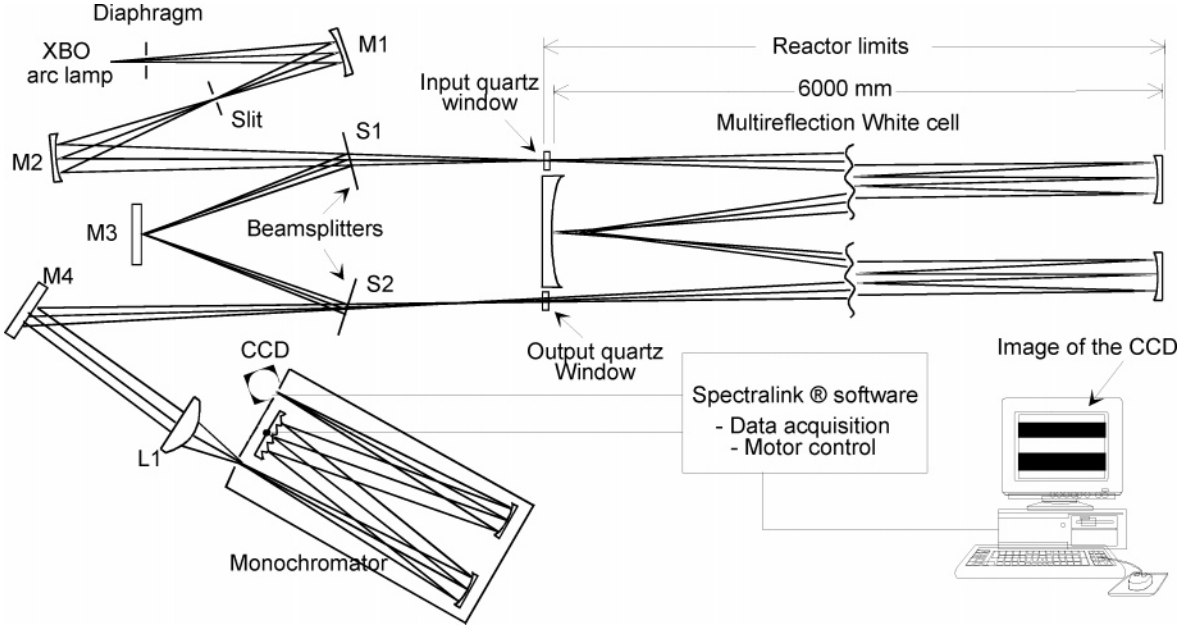

Figure 2. Optical setup of the UV−visible channel.

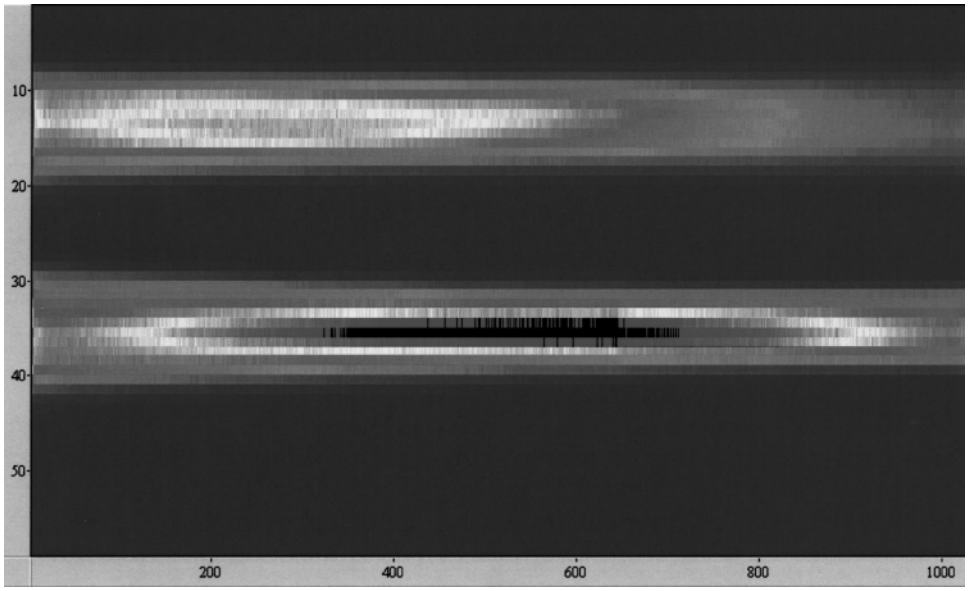

Figure 3. Signal view on the CCD. The upper beam corresponds to the one entering in the optical cell, and the lower beam corresponds to the one staying outside.

turbomolecular pumps to remove all residual molecules which may have remained adsorbed on the walls of the reactor. This cleaning procedure was performed to prevent any chemical ozone loss during the spectra acquisition and any UV and/or IR absorption from residual or formed compounds. As a result, no residual compound has been detected in the spectra of this study.

During the experiments, the reactor was filled with pure nitrogen (from liquid nitrogen evaporation, ≥99.995%, Linde) at atmospheric pressure and infrared and UV reference spectra were acquired. Then, a few millibars of the O_3/O_2 mixture were introduced in the reactor and mixed using fans inside the vessel. Gaseous ozone was generated in a discharge generator (OSRAM) that produces 0.5% of ozone in pure O_2 (N45, ≥99.99%, Air Liquide). It should be noticed that, using this method, the concentration of ozone in the reactor is not precisely known. However, this is not a problem in our case since the main goal of this study was to perform an intercomparison of UV and infrared ozone absorption coefficients, and not to determine absolute absorption cross-sections or line intensities. Finally, UV and infrared absorption spectra of ozone were simultaneously recorded, and the absorbances were obtained by calculating $\ln(I_0/I)$.

It is worth stressing that, with the UV "divided-beam" system (see Figure 2), the absorbance in the UV region is determined using a specific procedure:

(i) After the reactor has been filled with nitrogen, reference spectra, $(I_0)_{in}$—the spectrum of the UV beam passing through the cell filled only with N_2—as well as $(I_0)_{out}$—the spectrum of the UV beam passing through the reference optics mounted in front of the cell—are simultaneously acquired.

(ii) A transfer function F is calculated as $F = (I_0)_{in}/(I_0)_{out}$, which is the ratio of the spectral throughputs of the empty cell and of the reference optics in front of the cell.

(iii) After the ozone sample has been introduced into the reactor, the absorption spectrum $(I)_{in}$ and a new reference spectrum $(I)_{out}$ are simultaneously acquired.

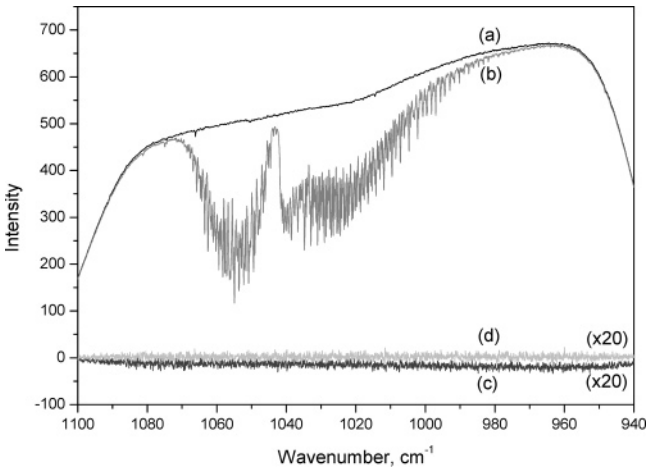

Figure 4. Infrared spectra with (I) and without (I_0) ozone, source off and source on: (a) I_0, source on; (b) I, source on; (c) I_0, source off; (d) I, source off.

(iv) A "virtual" $(I_0)_{vir}$ reference spectrum of the empty cell corresponding to the one that would have been measured without ozone at the time when the spectrum $(I)_{in}$ has been acquired, is calculated using the transfer function: $(I_0)_{vir} = F(I)_{out}$.

(v) Finally, the absorbance is calculated using $A = \ln((I_0)_{vir}/(I)_{in})$.

This procedure has the very important advantage of taking into account variations or drifts of the output of the xenon arc lamp. Such drifts are well-known and would cause systematic errors in the UV, where the ozone absorption is continuous and where it is not possible to determine variations in the I_0 base line from the absorption spectrum itself, in contrast to the infrared region where the ozone absorption is zero outside of the vibrational bands.

2.3. Wavelength Calibration in the UV Region. The wavelength scale of the UV−visible spectrometer was calibrated with reference to 15 emission lines of mercury, zinc, and cadmium between 300 and 360 nm. In this way the wavelength precision is observed to be better than 0.03 nm. The CCD detector enables us to acquire spectra during the experiments and wavelength calibrations without moving the monochromator, thus eliminating errors due to wavelength shifts resulting from mechanical backlash of the monochromator.

2.4. Correction for Sample Emission in the Infrared. To detect possible systematic intensity errors caused by sample and window thermal emissions,[18,19] FTIR spectra with the infrared light source switched off were recorded both with and without ozone in the cell. In all cases, no signal different from noise was detected, indicating that thermal radiation does not lead to systematic infrared absorption errors in the present experimental setup (see Figure 4).

3. Results

Eight intercomparison experiments using different experimental conditions were performed by simultaneously acquiring UV and IR spectra, leading to an average of 15 UV/IR data sets. Figure 5 shows an example of these spectra acquired with a UV and IR path length of 72 and 60 m, respectively, and with an ozone concentration of about 16 ppm. As a first step the recorded spectra were compared to those published in the literature in order to identify potential artifacts (impurities, saturation, etc.). As an example Figure 6a presents such a comparison in the UV region: a spectrum of the present study is compared (after convolution by the apparatus function of the present setup; see above) to a reference spectrum measured at high resolution by Malicet et al.[12] It can be seen that no significant deviation is observed between 300 and 320 nm. Above 320 nm, the agreement is less satisfactory since the measured absorbances are rather low (<0.1) and therefore sensitive to small base-line drifts. Consequently only UV data from 300 to 320 nm were used for the intercomparisons. Figure 6b shows the excellent agreement between another spectrum of this study and the data of Malicet et al.[12] In a similar fashion, in the infrared region, the spectra of the present study were compared to simulated spectra calculated using the HITRAN line parameters database[20] after convolution by the apparatus function (approximated by a Lorentzian line shape). In Figure 7, an example of this comparison is presented: the agreement between the two spectra is very good, showing in particular the absence of impurities and only small residuals that are only due to the nonperfect modeling of the FTIR apparatus function.

Having verified the quality of the UV and infrared spectra, one can now compare the UV and infrared absorption coefficients. For this purpose the ratios $(\int(A\,d\sigma)l)_{IR}/(A_\lambda l)_{UV}$ (where A and l are respectively the absorbances and the optical path lengths) were calculated for the various experiments. To get rid of possible UV wavelength calibration errors, such ratios were calculated for various UV wavelengths corresponding to reference spectral lines of Hg, Zn, or Cd, namely, those at 302.15, 307.59, 308.08, 312.57, and 313.17 nm. In the infrared region, the measured absorbances were integrated between 950 and 1085 cm^{-1}. Examples of IR/UV calibration plots are shown in Figure 8, and the corresponding results are presented in Table 1.

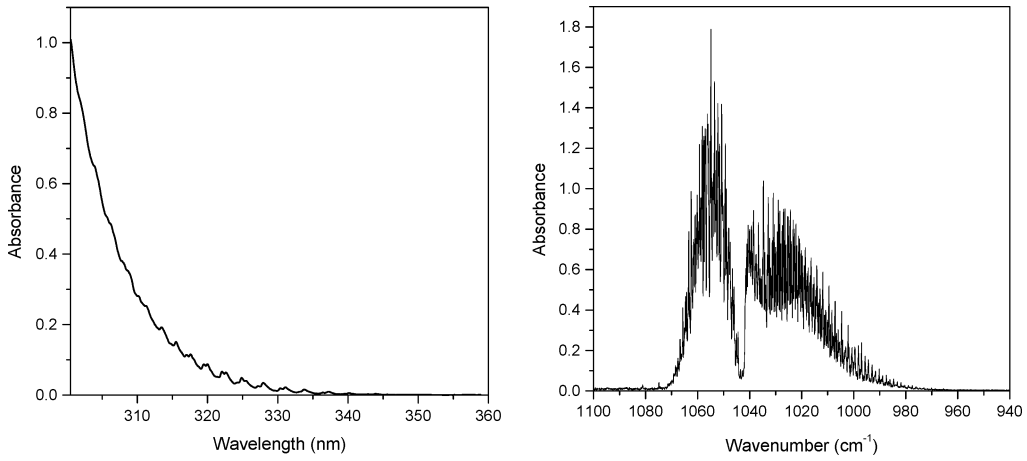

Figure 5. Example of UV and IR spectra of ozone acquired simultaneously.

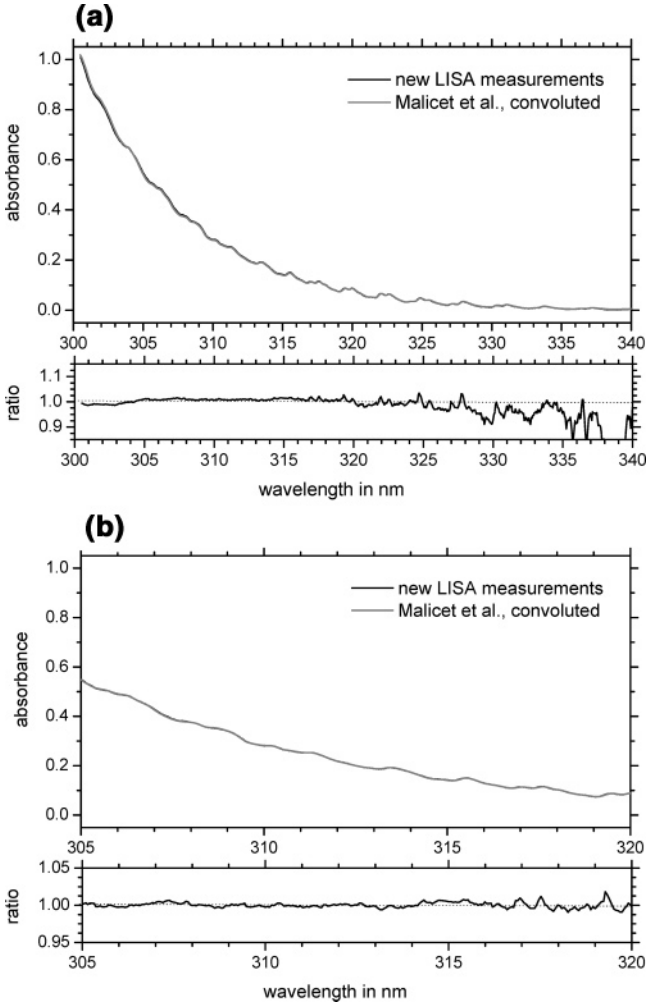

Figure 6. Comparison of UV spectra acquired by Malicet et al. and by this work.

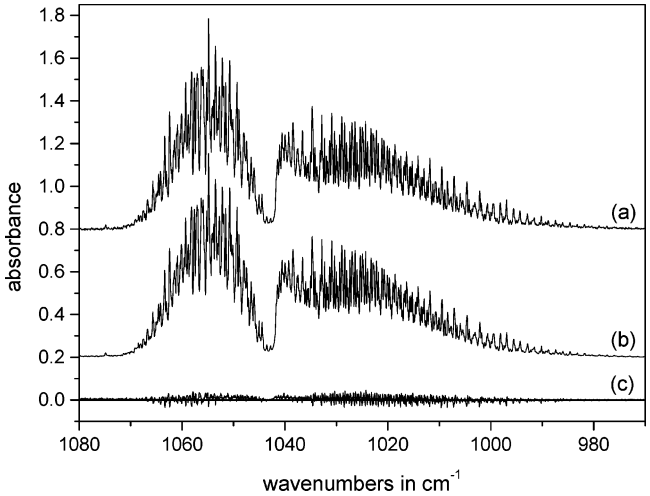

Figure 7. Comparison of IR spectrum acquired by this work (a) with theoritical spectrum calculated from the HITRAN database (b). Plot c corresponds to a − b.

These ratios were then compared to the various ratios IBI_{IR}/σ_{UV} one can obtain when using infrared integrated band intensities (IBI_{IR}) and UV absorption cross-sections σ_{UV} published in the literature. The results are presented in Table 2. In Table 3 we give the relative differences (%) between the IR/UV ratios measured in this work and the IR/UV ratios derived from the literature values.

TABLE 1: Experimental IR/UV Absorption Ratios

λ_{UV} (nm)	$(\int(A\,d\sigma)l)_{IR}/(A_\lambda l)_{UV}$[a]
302.15	52.3 ± 1.2[b]
307.59	111.9 ± 2.6[b]
308.08	115.5 ± 2.7[b]
312.57	217.6 ± 2.2[b]
313.17	230.4 ± 2.5[b]

[a] Spectral range [950−1085 cm^{-1}]. [b] Indicated experimental errors correspond to a 2σ standard deviation.

Finally, to verify that choosing selected UV wavelengths does not induce systematic errors, a calculation was performed using the entire UV spectrum for one of the eight experiments and for one published infrared band intensity (data set 1, Malicet et al./HITRAN 2000): after having convoluted the spectrum of Malicet et al. with the apparatus function of the present setup, the coefficient $[O_3]l$ (with $[O_3]$ being the ozone concentration in the reactor and l the optical path length of the UV pathway) that allows fitting of our absorbance spectrum was determined in the 305−320-nm region. As can be seen in Figure 6b, the agreement between the two spectra is excellent in this region, confirming that choosing selected wavelengths does not induce any systematic errors.

4. Discussion

From the results of Tables 2 and 3 it appears that, on the average, the HITRAN cross-sections and those derived from the review of Flaud et al.[8] are about 1.2 and 5.3% lower, respectively, than the values derived from our experiments assuming that the UV cross-sections are correct. The internal consistency of the data of the present study is very good, about 1%, showing that the linearity of absorption was clearly fulfilled (no error was introduced due to the limited spectral resolution of the UV spectrometer).

Now looking at the results one can make the following observations:

(i) The experimentally determined ratios (see Table 1) are on average known to better than 1.8%.

(ii) The available UV cross-sections in the Huggins bands are accurate to at least 1−2%,[1] and this is also clearly observed in the highly consistent ratios of this study (0.3% variation when discarding the data of Bogumil et al.[21]).

(iii) The infrared cross-sections at 10 μm are estimated to be known to within 1.8%,[8] but systematic differences of up to 4% have been observed between different laboratory studies that are clearly reflected in the IR/UV ratios of this study.

Although the present set of experiments seems to prove that an excellent consistency exists between the recommended UV cross-sections in the 300−320-nm spectral region[9,12,13] and the HITRAN 2000 band intensities at 10 μm (as well as with the IR/UV study of Smith et al.[5]), one cannot yet conclude for sure that the infrared line intensities derived from the review of three independent infrared measurements at 10 μm[4,6,7] are incorrect. Nevertheless, at the same time, it is important to note that, in the present study, several sources for systematic errors have been avoided: drifts of the xenon arc lamp in the UV (using the simultaneous reference measurements), wavelength calibration errors (using only wavelengths that correspond to atomic lines that have been employed for spectral calibration), nonlinearity of the absorbance (using a range of different path lengths and sample concentrations), determination of the ozone partial pressure (using only the ratios of IR and UV absorptions), and infrared sample emission (by recording spectra without the IR light source), etc. Also, it seems quite impossible that the

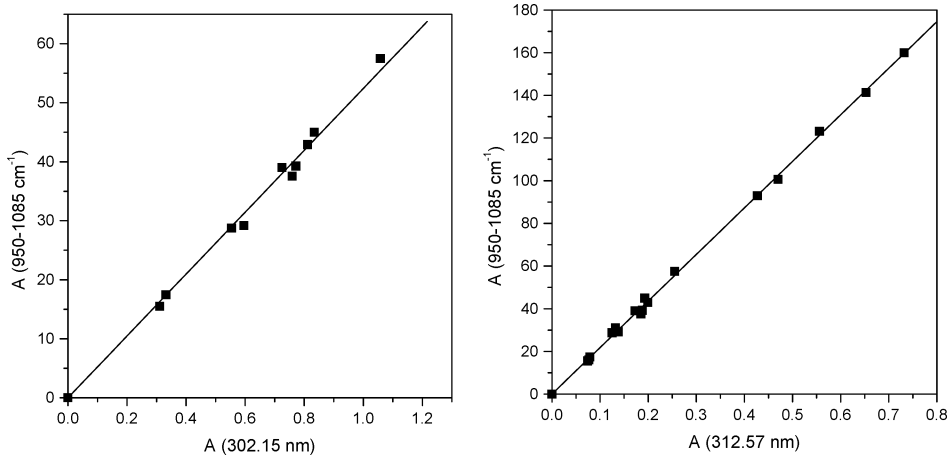

Figure 8. IR/UV calibration plots.

TABLE 2: Comparison of IR/UV Absorption Ratios Obtained by This Study with the Ratios IBI_{IR}/σ_{UV} Derived from the Literature

		for given lit. data set[a]							
λ_{UV} (nm)	this work	**1**	**2**	**3**	**4**	**5**	**6**	**7**	**8**
302.15	52.3	51.3	51.6	51.9	51.2	49.3	49.6	49.8	49.2
307.59	111.9	110.6	110.5	112.2	110.3	106.3	106.1	107.8	106.0
308.08	115.5	113.6	113.7	115.4	113.2	109.1	109.2	110.9	108.7
312.57	217.6	214.3	215.8	217.0	214.6	205.9	207.3	208.5	206.2
313.17	230.4	226.3	226.3	229.4	227.3	217.5	217.5	220.4	218.4

[a] Literature data sets: (1) HITRAN 2000/Malicet et al., 1995; (2) HITRAN 2000/Bass and Paur, 1985; (3) HITRAN 2000/Bogumil et al., 2001; (4) HITRAN 2000/Burrows et al., 1999; (5) Flaud et al., 2003/Malicet et al., 1995; (6) Flaud et al., 2003/Bass and Paur, 1985; (7) Flaud et al., 2003/Bogumil et al., 2001; (8) Flaud et al., 2003/Burrows et al., 1999.

TABLE 3: Differences (%) between IR/UV Absorption Ratios Measured in This Study and the IBI_{IR}/σ_{UV} Ratios Derived from Literature Values

	for given lit. data set[a]							
λ_{UV} (nm)	**1**	**2**	**3**	**4**	**5**	**6**	**7**	**8**
302.15	1.88	1.33	0.79	2.15	6.04	5.47	4.90	6.32
307.59	1.18	1.32	−0.21	1.47	5.31	5.46	3.86	5.61
308.08	1.68	1.60	0.09	2.05	5.83	5.75	4.18	6.22
312.57	1.57	0.86	0.29	1.43	5.72	4.98	4.38	5.57
313.17	1.78	1.78	0.42	1.33	5.93	5.93	4.52	5.46
average	1.62	1.38	0.28	1.69	5.76	5.52	4.37	5.84

[a] Literature data sets: (1) HITRAN 2000/Malicet et al., 1995; (2) HITRAN 2000/Bass and Paur, 1985; (3) HITRAN 2000/Bogumil et al., 2001; (4) HITRAN 2000/Burrows et al., 1999; (5) Flaud et al., 2003/Malicet et al., 1995; (6) Flaud et al., 2003/Bass and Paur, 1985; (7) Flaud et al., 2003/Bogumil et al., 2001; (8) Flaud et al., 2003/Burrows et al., 1999.

path length determination is wrong by as much as 4% for either the IR or UV beams or by 2% for each of the two beams (for the size of the reactor employed, this corresponds to 24 or 12 cm, respectively). But at the same time, it cannot be excluded that some unconsidered systematic error is still present and—at least in part—responsible for the discrepancies between the new measurements of this study and the infrared line intensities based on three independent studies. Another possibility, i.e., that the infrared and Huggins bands of ozone arise—at least partly—from different lower electronic or vibrational states, can be excluded on the basis of recent theoretical studies.[22] Thus, the discrepancies between several accurate laboratory measurements remain unexplained. Therefore, future measurements of the ozone absorption coefficients in the UV and IR regions are needed to resolve this important issue.

5. Conclusion

For the first time, a series of spectroscopic experiments for comparing the absorption coefficients of ozone in the UV (between 300 and 320 nm) and IR (around 10 μm) regions has been performed. The analysis shows good agreement (around 98.5%) between the HITRAN 2000 recommendation for the mid-infrared and the most referenced measurements in the ultraviolet regions, whereas systematic differences of about 5.5% are observed when using the recommendation of HITRAN 2003 for the mid-infrared. Future independent study measurements are clearly needed to resolve this issue.

Acknowledgment. The work presented in this paper was supported by the French National Program for Atmospheric Chemistry (PNCA). One of the authors (B.P.-V.) thanks the French National Space Agency (CNES) for a postdoctoral fellowship and Y. Benilan for his help.

References and Notes

(1) Orphal, J.; Chance, K. *J. Quant. Spectrosc. Radiat. Transfer* **2003**, *82*, 491.

(2) Pickett, H. M.; Peterson, D. B.; Margolis, J. S. *J. Geophys. Res.* **1992**, *97*, 20787.

(3) De Backer, M. R.; Parvitte, B.; Zeninari, V.; Courtois, D. *J. Quant. Spectrosc. Radiat. Transfer* **1995**, *54*, 1009.

(4) De Backer-Barilly, M. R.; Barbe, A. *J. Mol. Spectrosc.* **2001**, *205*, 43.
(5) Smith, M. A. H.; Devi, V. M.; Benner, D. C.; Rinsland, C. P. *J. Geophys. Res.* **2001**, *106*, 9909.
(6) Claveau, C.; Camy-Peyret, C.; Valentin, A.; Flaud, J. M. *J. Mol. Spectrosc.* **2001**, *206*, 115.
(7) Wagner, G.; Birk, M.; Schreier, F.; Flaud, J. M. *J. Geophys. Res.* **2002**, *107*.
(8) Flaud, J. M.; Wagner, G.; Birk, M.; Camy-Peyret, C.; Claveau, C.; De Backer-Barilly, M. R.; Barbe, A.; Piccolo, C. *J. Geophys. Res.* **2003**, *108*, 4269.
(9) Bass, A. M.; Paur, R. J. *The Ultraviolet Cross-Sections of Ozone, I: The Measurements*; D. Reidel: Norwell, MA, 1985.
(10) Molina, L. T.; Molina, M. J. *J. Geophys. Res.* **1986**, *91*, 14501.
(11) Brion, J.; Chakir, A.; Charbonnier, J.; Daumont, D.; Parisse, C.; Malicet, J. *J. Atmos. Chem.* **1998**, *30*, 291.
(12) Malicet, J.; Daumont, D.; Chardonnier, J.; Parisse, C.; Chakir, A.; Brion, J. *J. Atmos. Chem.* **1995**, *21*, 263.
(13) Burrows, J. P.; Richter, A.; Dehn, A.; Deters, B.; Himmelmann, S.; Voigt, S.; Orphal, J. *J. Quant. Spectrosc. Radiat. Transfer* **1999**, *61*, 509.
(14) Voigt, S.; Orphal, J.; Bogumil, K.; Burrows, J. P. *J. Photochem. Photobiol., A* **2001**, *143*, 1.
(15) Bogumil, K.; Orphal, J.; Burrows, J. P.; Flaud, J. M. *Chem. Phys. Lett.* **2001**, *349*, 241.
(16) Orphal, J. A Critical Review of the Absorption Cross-Sections of O_3 and NO_2 in the Ultraviolet and Visible. *J. Photochem. Photobiol., A* **2003**, *157*, 185.
(17) Doussin, J. F.; Ritz, D.; Durand-Jolibois, R.; Monod, A.; Carlier, P. *Analusis* **1997**, *25*, 236.
(18) Birk, M.; Hausamann, D.; Wagner, G.; Johns, J. W. *Appl. Opt.* **1996**, *35*, 2971.
(19) Ballard, J.; Remedios, J. J.; Roscoe, H. K. *J. Quant. Spectrosc. Radiat. Transfer* **1992**, *48*, 733.
(20) Rothman, L. S.; Barbe, A.; Benner, D. C.; Brown, N. R.; Camy-Peyret, C.; Carleer, M. R.; Chance, K.; Clerbaux, C.; Dana, V.; Devi, V. M.; Fayt, A.; Flaud, J. M.; Gamache, R. R.; Goldman, A.; Jacquemart, D.; Jucks, K. W.; Lafferty, J. W.; Mandin, J. Y.; Massie, S. T.; Nemtchinov, V.; Newnham, D. A.; Perrin, A.; Rinsland, C. P.; Schroeder, J.; Smith, K. M.; Smith, M. A. H.; Tang, K.; Toth, R. A.; Vander Auwera, J.; Varanasi, P.; Yoshino, K. *J. Quant. Spectrosc. Radiat. Transfer* **2003**, *82*, 5.
(21) Bogumil, K.; Orphal, J.; Homann, T.; Voigt, S.; Spietz, P.; Fleischmann, O. C.; Vogel, A.; Hartmann, M.; Bovensmann, H.; Frerick, J.; Burrows, J. P. *J. Photochem. Photobio., A Chem.* **2003**, *157*, 167.
(22) Qu, Z. W.; Zhu, H.; Tashiro, M.; Schinke, R.; Farantos, S. C. *J. Chem. Phys.* **2004**, *120*, 6811.